Separation Science and Technology
Publication details, including instructions for authors and subscription information:
http://www.informaworld.com/smpp/title~content=t713708471

Dehydration of Glycerol-Water Mixtures Using Pervaporation: Influence of Process Parameters

Keya Biswas[a]; Sayoni Datta[a]; Siladitya Chaudhuri[a]; Kajari Kargupta[a]; Siddhartha Datta[a]; Shyamal K. Sanyal[a]
[a] DEPARTMENT OF CHEMICAL ENGINEERING, JADAVPUR UNIVERSITY, CALCUTTA, INDIA

To cite this Article Biswas, Keya , Datta, Sayoni , Chaudhuri, Siladitya , Kargupta, Kajari , Datta, Siddhartha and Sanyal, Shyamal K.(2000) 'Dehydration of Glycerol-Water Mixtures Using Pervaporation: Influence of Process Parameters', Separation Science and Technology, 35: 9, 1391 — 1408

To link to this Article: DOI: 10.1081/SS-100100231

URL: http://dx.doi.org/10.1081/SS-100100231

SEPARATION SCIENCE AND TECHNOLOGY, **35**(9), pp.1391–1408, 2000

Dehydration of Glycerol–Water Mixtures Using Pervaporation: Influence of Process Parameters

---

KEYA BISWAS, SAYONI DATTA, SILADITYA CHAUDHURI,
KAJARI KARGUPTA, SIDDHARTHA DATTA, and
SHYAMAL K. SANYAL*
DEPARTMENT OF CHEMICAL ENGINEERING
JADAVPUR UNIVERSITY
CALCUTTA 700032, INDIA

ABSTRACT

Pervaporation, a membrane-based separation technique, is proposed as a potential replacement for the vacuum distillation process which is normally used for the dehydration of glycerol–water mixtures. Separation characteristics of glycerol–water mixtures containing a trace amount of water by using a water-selective cellophane membrane are studied. Experiments show that the membrane is selective toward water, and pure water is obtained as the permeant. Thus, the selectivity coefficient is infinite. However, the rate of permeation of water is solely controlled by the liquid-phase mass transfer boundary layer resistance due to the very high viscosity of glycerol. Accordingly, increased agitation and temperature cause considerable enhancement of flux. On the other hand, the presence of salt in the feed mixture significantly reduces the rate of permeation. An unsteady-state model, that includes various process parameters, has been developed for prediction of the process output. The model prediction fits satisfactorily with the experimental observations of the present study.

INTRODUCTION

The separation of binary mixture by pervaporation has received increasing attention over the past two decades. The perm-selective behavior of a membrane displaying a preferential affinity for one component is the basis for separation in pervaporation. The driving force for transport is the gradient in chemical potential across the membrane. This is maintained by lowering the

---

* To whom correspondence should be addressed.

www.dekker.com

downstream pressure below the vapor pressure of the components. In order to achieve this, the downstream side has to be kept under vacuum or under an inert stream. Unlike other membrane separation techniques, use of vacuum makes the process energy intensive, so it is mostly used for single-stage separation of liquid mixtures where conventional separation processes either fail completely or become highly energy consuming. The recent development of synthetic and composite membranes has made pervaporation potentially attractive for difficult-to-separate azeotrope, close boiling, and isomeric mixtures (1–7). Pervaporation is increasingly being considered as a potential replacement for such existing processes as distillation and adsorption for the dehydration and recovery of organic solvents. It has been found to be economic when water is present in trace amounts. Distillation becomes prohibitively expensive for the removal of a small amount of water. Although the capital cost of adsorption is usually low, operating costs, including adsorbent replacement, the high energy of regeneration, and adsorbent disposal are significant deterrents in many cases. Extensive research and commercialization of pervaporation in industry were done for the separation of trace amounts of water from such organics as alcohols, xylene, methyl ethyl ketone, etc. (8–12). Neel et al. (13) reported the separation of a water–tetrahydrofuran mixture using Cuprophan membrane. Separation of trace amounts of water from an octanol–water mixture using a hydrophilic cellulose membrane was investigated by Gref et al. (14).

In the soap and detergent industry the separation of the trace amounts of water present in glycerol is currently achieved by vacuum distillation. The resulting 99.9% glycerol is commercially important in the manufacture of drugs and pharmaceuticals and for creating dynamite. The outlet stream from a multiple effect evaporator containing around 80% glycerol and any remaining salt and water is then sent to a vacuum distillation unit (15). The process is energy intensive. Elimination of polymerization and decomposition of product limit the maximum operating temperature, as well as dictating the vacuum to be maintained. Furthermore, water, the more volatile component, is present in trace amounts. Thus, pervaporation using a highly water selective membrane may prove to be an alternative to the vacuum distillation process.

The present work studies the separation characteristics of glycerol–water mixtures containing trace amounts of water by pervaporation using water selective cellophane membranes. Attempts have been made in the present work to study the effect of temperature, external liquid phase agitation, feed composition, and the presence of salt in the feed on the permeation rates and separation characteristics.

The transport process in pervaporation has been described mostly in terms of the well-known solution-diffusion (16, 17) model. According to this model, the separation process is governed by the rate of sorption and diffusion of the components in the membrane and on the rate of desorption at the downstream side of the membrane. Because of the relatively low permeability of dense membranes, the mass transfer resistance in the external liquid phase is often neglected when accounting for the total resistance. However, in the present case glycerol is highly viscous and water present in trace amounts selectively passes through the membrane. As mentioned by Gref et al. (14), when the component extracted by the membrane in pervaporation is present at trace levels in the bulk of the feed solution and its flux is sufficiently high, this component may be so depleted at the membrane surface that transport in the boundary layer becomes the rate-limiting step and completely controls the behavior of the membrane system. The phenomenon is often termed "concentration polarization." Cote and Lipski (18) accounted for the latter by using a resistances-in-series model. Gref et al. (14) studied the influence of concentration polarization on the dehydration of octanol–water mixtures by using a steady-state resistances-in-series model. Heintz et al. (19) studied the influence of concentration polarization using a generalized solution-diffusion model. For prediction of the rate of permeation and the time required for removal of water, an unsteady-state model has been developed that considers both the liquid phase and membrane phase resistances. The simulation parameters used in the present model were experimentally determined, and therefore no adjustable parameter is used.

EXPERIMENTAL

Materials

The membrane used was commercially available cellophane film (PT 300 of Kesoram Rayon Ltd., India, thickness 0.025 mm, density 1.41 $g \cdot cm^{-3}$). Total membrane area was 0.0038 m^2. Double distilled water and glycerol (A.R. grade) of refractive indices 1.33 and 1.466, respectively, at 30°C were used. Glycerol was obtained from Ranbaxy Laboratories Ltd., India.

Analysis

The feed and the permeate compositions were analyzed at 30°C by measuring the refractive indices with an Abby-type refractometer (Erma, Japan).

Pervaporation Apparatus

The batch unsteady-state pervaporation runs were carried out in a permeation cell as shown in Fig. 1. The cell consisted of two 12.25 cm o.d. and 8.8 cm i.d. aluminum flanges. The membrane was supported by a porous aluminum disk of sufficient porosity. The upper compartment or the feed cham-

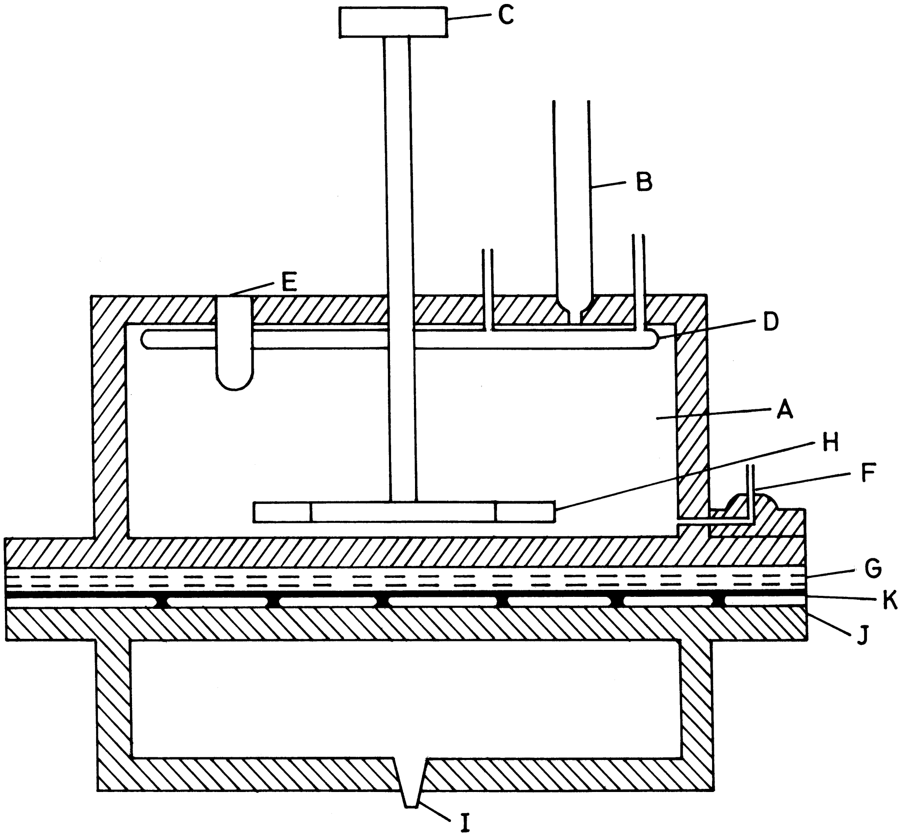

FIG. 1 Pervaporation cell. A: Feed chamber. B: Condenser. C: Variable speed motor. D: Hot water circulation coil. E: Thermowell. F: Precision bore capillary tube. G: Rubber gasket. H: Stirrer. I: Vapor removal tube. J: Porous aluminum disk. K: Membrane.

ber was 1.5 cm deep and was fitted with a thermowell for measuring the temperature of the feed. It was also provided with a glass condenser for minimizing loss of material through evaporation. The temperature control of the feed charge was monitored by circulating hot water at the required temperature through a copper heating coil immersed in the feed compartment. The water was circulated through the coil by a pump submerged in a thermostatic water bath. The temperature in the water bath was maintained within ±0.5°C of the set temperature.

For agitation in the feed compartment, a stainless steel paddle wheel fitted to a variable speed motor was used. The speed of agitation was measured using a tachometer.

Procedure

The permeation cell holding the cellophane membrane was bolted together. After making the necessary connections to the cold trap, the pressure gauge, and the vacuum pump, the system was evacuated for half an hour at pressure between 4–7 mmHg and tested for leaks. Hot water was then circulated from the thermostatic water bath through the heating coil, and a constant temperature was maintained in the feed chamber. A feed mixture of specified composition of glycerol and water (certain runs also contained common salt) was then introduced into the feed chamber. Vapor permeant was condensed and was collected at regular intervals in the trap that was immersed in a Dewar flask. The Dewar flask was filled with liquid nitrogen. The permeation rate was measured by weighing the amount collected over a given period. The collected permeate was allowed to attain 30°C and then analyzed.

Sorption Measurement

The cellophane membrane was allowed to equilibriate pure water at a specified temperature. The resulting weight gain by the membrane gives the total sorption of water, i.e., the composition of water in the membrane at equilibrium (C_w^m). The same experiment with pure glycerol gives the values of C_g^m.

RESULTS AND DISCUSSION

The experimental result shows that over a wide range of process parameters, viz., temperature, speed of agitation, and feed concentration, pure water permeates through the membrane with no trace of glycerol. Thus the selectivity coefficient λ, defined as $y_w x_g / y_g x_w$, is ∞. Table 1 shows the solubility of pure water and pure glycerol in the cellophane membrane as obtained from the sorption experiment at 30°C. Thus, although glycerol is sorbed by the membrane, it can not permeate through the membrane.

The important process parameters which may influence the rate of permeation of a component in pervaporation are feed concentration, feed tempera-

TABLE 1
Properties of Glycerol, Water, and Cellophane

	Component		
Property	Glycerol	Water	Cellophane
Molecular weight	92.11	18.00	—
Boiling point (°C)	120 at 20 atm	100 at 1 atm	—
Density (g/cm^3)	1.2613	1.0000	1.41.00
Molar volume (cm^3/mol)	73.02	18.00	—
Refractive index (30°C)	1.466	1.331	—
Solubility (mol/cm^3)	4.036×10^{-3}	0.025	—
$g_{i\text{-polymer}}$	1.0354	0.8124	—

ture, downstream pressure, and the external phase agitation. However, since water permeates in the present case as a pure component and the downstream pressure is maintained very low (4–7 mmHg), its effect on the overall permeation rate is negligible. The remaining three parameters have a pronounced effect on the external transport as well as on transport through the membrane.

Figure 2 shows the experimental cumulative weight of product vs time data, obtained by using an unstirred batch cell at various temperatures. The flux data at different temperatures were obtained from the slopes of the curves and are plotted in Fig. 3. Figure 4 shows the experimental flux vs time data, obtained from a stirred cell at 43°C for different agitator speeds. It can be inferred from Figs. 2 and 3 that the initial rate of permeation of water is highly enhanced by an increase in temperature from 36.5 to 50°C, although the increase in the steady-state rate is not significant beyond 43°C. Figure 4 shows the rate of permeation increase with an increase in the agitator speed. Figure 5 shows the effect of a change of feed concentration on the flux of water. The results show a considerable enhancement of the rate of permeation with a decrease in glycerol concentration in the feed from 80 to 50%.

Based on the above observations it can be inferred that external liquid phase mass transfer plays an important role on the overall rate of transport of water. Water, the component separated by the membrane, is present in a trace amount

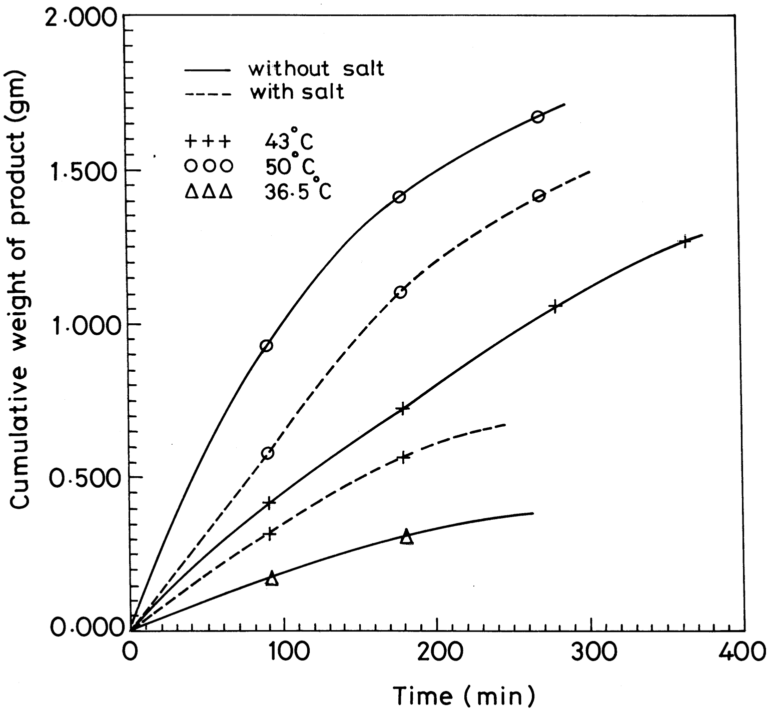

FIG. 2 Cumulative weight of product (g) vs time (minutes): Effect of bulk feed temperature and salt.

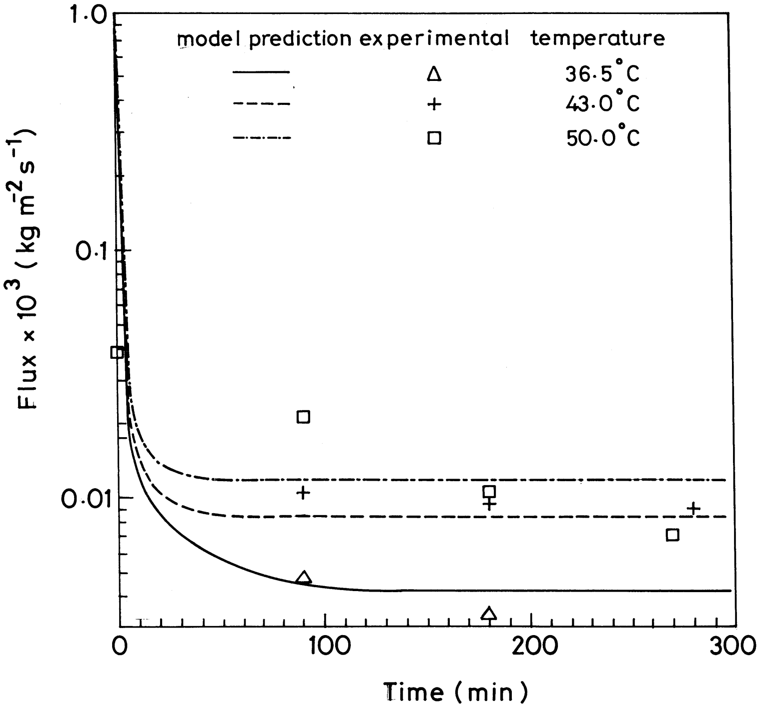

FIG. 3 Flux of water (kg·m^{-2}·s^{-1}) vs time (minutes): Effect of temperature.

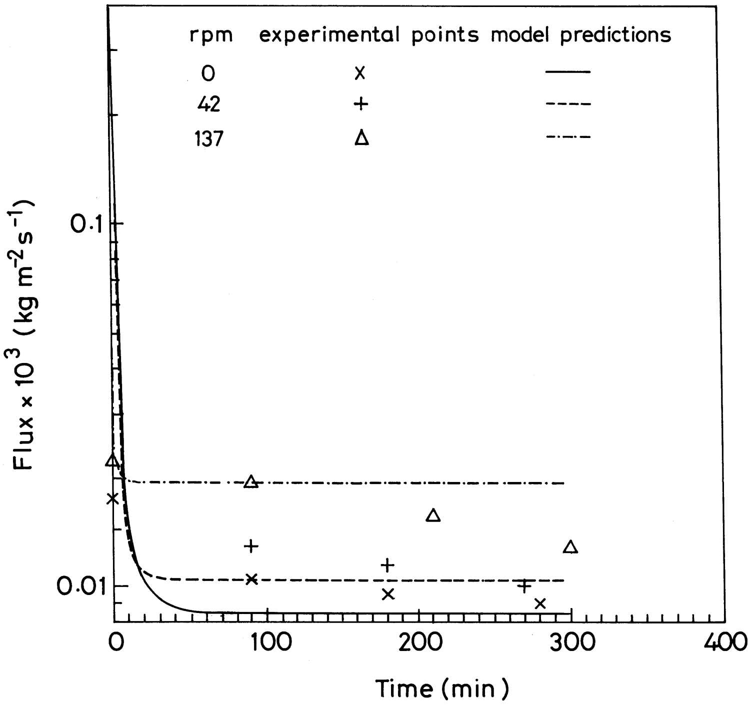

FIG. 4 Flux of water (kg·m^{-2}·s^{-1}) vs time (minutes): Effect of agitation.

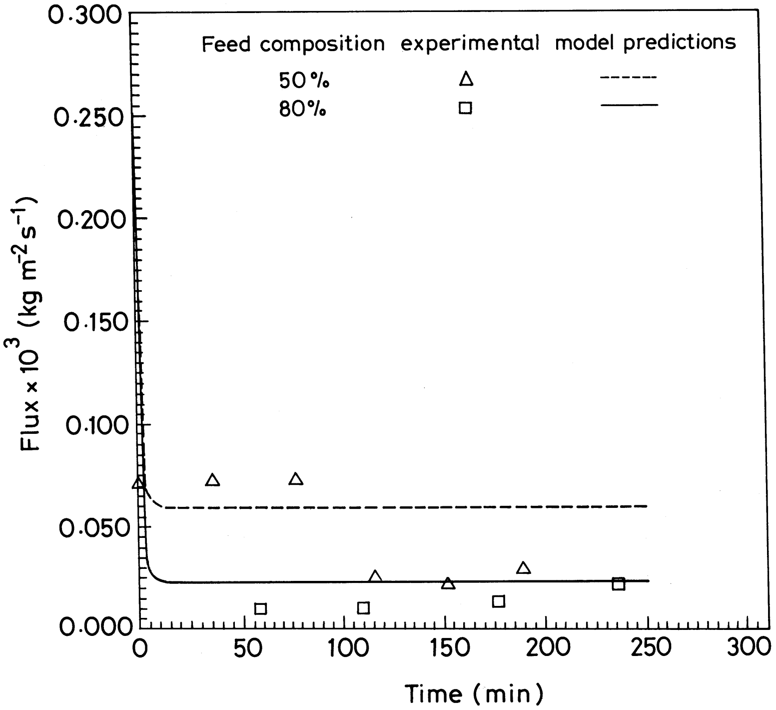

FIG. 5 Flux of water ($kg{\cdot}m^{-2}{\cdot}s^{-1}$) vs time (minutes): Effect of feed concentration.

in the bulk feed solution and its flux is significantly high through cellophane. The very high viscosity of glycerol results in a decrease in the diffusivity of water through glycerol. Thus, depletion of water at the membrane surface and the very low rate of diffusion of water through the bulk feed to the interface make transport in the boundary layer the limiting step. An increase in the speed of agitation sharply reduces the concentration boundary layer thickness (δ_c) and increases the rate of permeation. The increase in pervaporation flux with temperature is well established in the literature and is generally accounted for by the Arrhenius equation. However, in the present case the sharp reduction in the viscosity of glycerol with an increase in temperature greatly reduces the external phase resistance. The membrane phase resistance is also decreased due to an increase in permeability according to the Arrhenius relationship. A decrease in glycerol concentration in the feed effectively reduces mass transfer boundary layer resistance due to a lowered viscosity value. As a result, the rate of permeation increases.

Model Development

In order to estimate and verify the effect of process parameters on the rate of permeation, a simplified unsteady-state model has been established for the transport of solute under a concentration polarization regime.

The general unsteady-state model equation for the transport of water in the boundary layer can be written as

$$\frac{\partial C_{\mathrm{w}}}{\partial t} = D_{\mathrm{wg}} \frac{\partial^2 C_{\mathrm{w}}}{\partial z^2} \tag{1}$$

The initial and boundary conditions are:

$$C_{\mathrm{w}} = C_0,\ t = 0,\ \delta_{\mathrm{c}} \leq z \leq 0 \tag{2}$$

$$C_{\mathrm{w}} = C_0,\ t = t,\ z = \delta_{\mathrm{c}} \tag{3}$$

$$-D_{\mathrm{wg}} \frac{\partial C_{\mathrm{w}}}{\partial z} = n_{\mathrm{w}},\ t = t,\ z = 0 \tag{4}$$

For pure water permeation, the flux through the membrane can be written as

$$n_{\mathrm{w}} = \frac{D_{\mathrm{wg}}}{\delta_{\mathrm{m}}} (C_{\mathrm{w}}^{\mathrm{u}} - C_{\mathrm{w}}^{\mathrm{d}}) \tag{5}$$

$C_{\mathrm{w}}^{\mathrm{u}}$ and $C_{\mathrm{w}}^{\mathrm{d}}$ are related to the bulk concentrations by the equilibrium relationships:

$$x_i \gamma_i P_i^{\mathrm{sat}} = \alpha_i^{\mathrm{u}} C_i^{\mathrm{u}} \tag{6}$$

$$f_i y_i P^{\mathrm{d}} = \alpha_i^{\mathrm{d}} C_i^{\mathrm{d}} \tag{7}$$

Assume $\alpha^{\mathrm{u}} = \alpha^{\mathrm{d}}$, and substitute in the expression for flux (Eq. 5):

$$n_{\mathrm{w}} = \frac{D_{\mathrm{wg}}}{\alpha \delta_{\mathrm{m}}} (x_{\mathrm{w}} \gamma_{\mathrm{w}} P_{\mathrm{w}}^{\mathrm{sat}} - f_{\mathrm{w}} y_{\mathrm{w}} P^{\mathrm{d}}) \tag{8}$$

In terms of pure water permeability, Eq. (8) may be written as

$$n_{\mathrm{w}} = \beta \kappa (x_{\mathrm{w}} \gamma_{\mathrm{w}} P_{\mathrm{w}}^{\mathrm{sat}} - f_{\mathrm{w}} y_{\mathrm{w}} P^{\mathrm{d}}) / (\delta_{\mathrm{m}} V_{\mathrm{w}}) \tag{9}$$

where κ is the permeability of pure water through the membrane and β is the factor used to correct the solubility of water in the membrane due to the presence of glycerol. Since water permeates through the membrane as a pure component, diffusivity of water through the membrane is assumed to be independent of glycerol concentration:

$$\beta = \alpha_0 / \alpha \tag{10}$$

where α_0 is the equilibrium constant for pure water.

Estimation of Model Parameters

Pure Water Permeability

Pure water permeability may be related to the temperature by the well-known Arrhenius relation (20):

$$\kappa = \kappa_0 \exp(-E/RT) \tag{11}$$

For pure water permeation the flux equation becomes

$$n_{\mathrm{w}} = \kappa(P_{\mathrm{w}}^{\mathrm{sat}} - P^{\mathrm{d}})/(\delta_{\mathrm{m}} V_{\mathrm{w}}) \tag{12}$$

The rate of permeation of pure water at 36.5, 43, and 50°C has been obtained experimentally. By using these experimental data in the above equation, κ is obtained as a function of temperature. Figure 6 shows $\ln(\kappa)$ as a function of $1/T$. The calculated values of κ_0 and E/R are, respectively, 0.65227 $\mathrm{cm^3(stp)cm \cdot cm^{-2} \cdot s^{-1}(cmHg)^{-1}}$ and 5322 K.

Estimation of β

According to Eqs. (6) and (10), β may be expressed as

$$\beta = \left(\frac{x_{\mathrm{w}}\gamma_{\mathrm{w}}P_{\mathrm{w}}^{\mathrm{sat}}}{C_{\mathrm{w}}^{\mathrm{m}}\alpha_0}\right)^{-1} \tag{13}$$

α_0 for pure water is obtained from sorption experiments.

The equilibrium sorption concentration of water in the membrane, $C_{\mathrm{w}}^{\mathrm{m}}$, is obtained theoretically at any feed concentration by using Flory–Huggins thermodynamics (21). At sorption equilibrium:

$$\Delta\mu_{\mathrm{w}}^{1} = \Delta\mu_{\mathrm{w}}^{\mathrm{m}} \tag{14}$$

$$\Delta\mu_{\mathrm{g}}^{1} = \Delta\mu_{\mathrm{g}}^{\mathrm{m}} \tag{15}$$

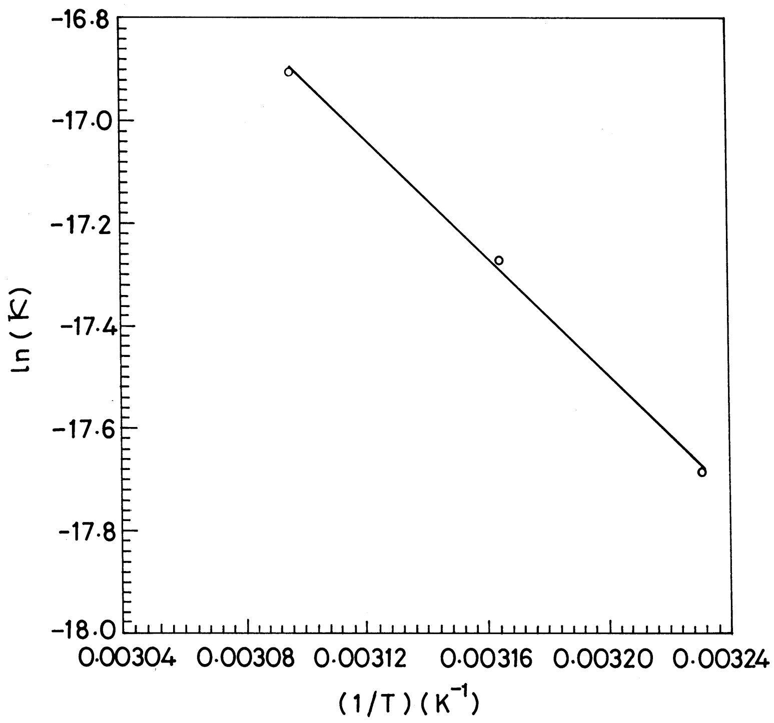

FIG. 6 Arrhenius plot: ln κ vs 1/T.

Following Mulder et al. (23, 24), $\Delta\mu_w^m$ and $\Delta\mu_g^m$ are expressed in terms of v_1, v_2, v_3 and of g_{12}, g_{13}, g_{23}:

$$\varphi_1(v_1, v_2, v_3, g_{12}, g_{13}, g_{23}) = 0 \tag{16}$$

$$\varphi_2(v_1, v_2, v_3, g_{12}, g_{13}, g_{23}) = 0 \tag{17}$$

The final forms of φ_1 and φ_2 are given in Appendix I. Original Flory–Huggins interaction parameters are used in the present case instead of concentration-dependent interaction parameters. The values of g_{13} and g_{23} are calculated by inserting the experimentally obtained pure water and pure glycerol equilibrium sorption data into the Flory–Rehner equation (21):

$$\ln(1 - v_p) + v_p + g_{ip}v_p^2 + \frac{V_i}{M_c V_p}(v_p^{0.333} - 0.5v_p) = 0 \tag{18}$$

The values obtained are given in Table 1. The binary interaction parameter g_{12} is evaluated from

$$g_{12}^1 = \frac{1}{x_1 u_2}\, x_1 \ln\left(\frac{x_1}{u_1}\right) + x_2 \ln\left(\frac{x_2}{u_2}\right) + \frac{\Delta G^E}{RT} \tag{19}$$

The excess Gibbs free energy data as well as the activity coefficient γ for water and glycerol are calculated using the group contribution method of UFAC (24). Substitution of g_{12}, g_{13}, and g_{23} in Eqs. (16) and (17) and simultaneous solution of these two nonlinear algebraic equations using the constraint $v_1 + v_2 + v_3 = 1$ gives the equilibrium sorption concentration of water and glycerol in cellophane. Figure 7 shows a plot of water sorbed concentration in cellophane as a function of glycerol concentration in feed at 30°C. By inserting the sorbed concentration of water $C_w^m\alpha$, γ_w, and P_w^{sat} data in Eq. (13), β may be obtained for different process conditions.

Estimation of δ_c

Estimation of the concentration boundary layer is necessary in order to solve Eq. (1). In the case of an unstirred batch cell, the momentum boundary layer thickness will be infinite. However, in the present case the depth of the total liquid present in the cell represents the momentum boundary layer thickness. In the case of flow over a parallel plate for molecular transport, the concentration boundary layer thickness δ_c is related to the momentum boundary layer thickness δ by

$$\delta_c/\delta = N_{Sc}^{-0.33} \tag{20}$$

However, the flow of liquid in this case, which is induced by diffusion, is not ideally parallel to the surface.

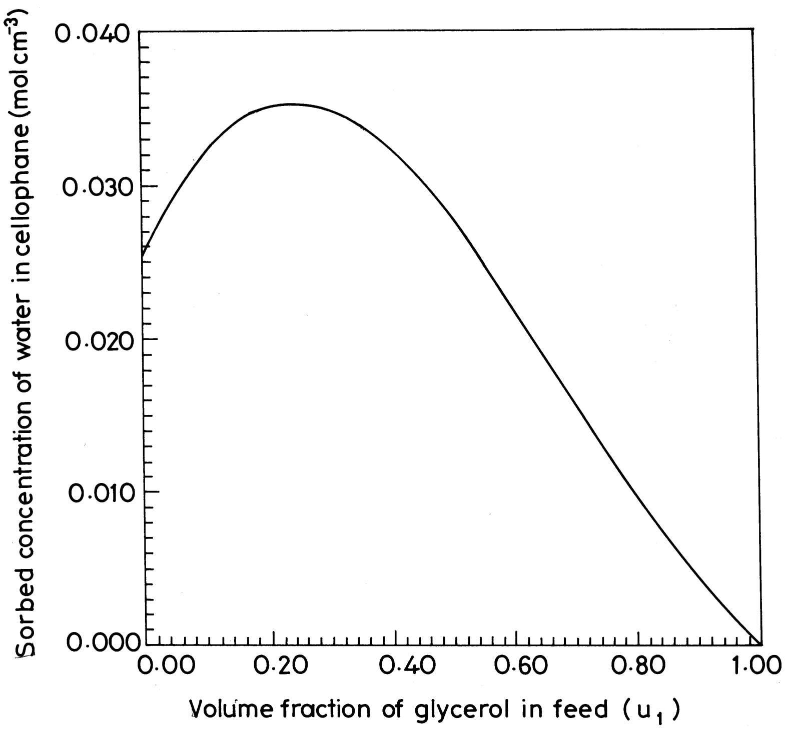

FIG. 7 Concentration of water in the membrane ($\mathrm{mol \cdot cm^{-3}}$) vs glycerol composition in the feed (u_1).

The value of the concentration boundary layer thickness δ_c can be obtained by using the film theory of mass transfer:

$$\delta_c = D/K \tag{21}$$

For a stirred batch cell the mass transfer coefficient can be determined using the expression of the Sherwood number:

$$N_{\mathrm{Sh}} = \theta_1(N_{\mathrm{Re}}, N_{\mathrm{Sc}}) \tag{22}$$

whereas for an unstirred cell:

$$N_{\mathrm{Sh}} = \theta_2(N_{\mathrm{Sc}}) \tag{23}$$

The general correlations available in the literature for Eq. (22) are mostly of the form

$$N_{\mathrm{Sh}} = aN_{\mathrm{Re}}^{\mathrm{b}}N_{\mathrm{Sc}}^{\mathrm{c}} \tag{24}$$

In the case of molecular transport, the value of "c" is mostly reported as 0.33. However, for the dissolution of solids in a turbine agitated vessel, the exponent "c" was found to be 0.5.

In order to develop the above correlation, experimental steady-state flux data were used to evaluate the Sherwood number at different Reynolds numbers and Schmidt numbers. At steady state:

$$n_{\mathrm{w}} = KC(x_{\mathrm{w}0} - x_{\mathrm{w}i}) = \frac{\kappa\beta}{\delta_{\mathrm{m}} V_{\mathrm{w}}}(\gamma_i x_{\mathrm{w}i} P_{\mathrm{w}}^{\mathrm{sat}} - y_{\mathrm{w}} P^{\mathrm{d}}) \tag{25}$$

Thus, using the resistances-in-series model, the steady-state equation becomes

$$n_{\mathrm{w}} = \frac{x_{\mathrm{w}0} - y_{\mathrm{w}} P^{\mathrm{d}}/\gamma_i P_{\mathrm{w}}^{\mathrm{sat}}}{\left[\dfrac{V_{\mathrm{w}}\delta_{\mathrm{m}}}{\beta\kappa\gamma_i P_{\mathrm{w}}^{\mathrm{sat}}} + \dfrac{1}{KC}\right]} \tag{26}$$

Substituting the experimental steady-state flux data (n_{w}) obtained at different temperatures, agitator speeds, and feed compositions, different values of the Sherwood number at different Reynolds numbers and Schmidt numbers are obtained. By using the multiple regression technique, the final form of the equation obtained is

$$N_{\mathrm{Sh}} = 0.02176 N_{\mathrm{Re}}^{0.4956} N_{\mathrm{Sc}}^{0.5} \tag{27}$$

For an unstirred cell the mass transfer coefficients are obtained by using the steady-state flux data in Eq. (26). For simulation, δ_{c} is directly obtained using Eq. (21) in the case of an unstirred cell, whereas it has been calculated from the above correlation for the stirred condition.

Simulation

The diffusivity of water in glycerol used for the simulation has been calculated using the Wilke–Chang equation (25).

Figures 3, 4, 5 show the results of simulation along with the experimental data. It is seen that the time required to attain steady state as predicted by the model is less than that obtained experimentally. The initial flux is found to be very high, which decreases sharply with time and attains a steady-state value which is almost the same as that obtained experimentally. The deviation of the experimental data from the theoretical flux data in the initial period is probably due to the lack of a large enough number for the cumulative weight of product vs time data in the initial period where the flux changes rapidly.

To summarize the effect of process parameters on the rate of permeation, the simulated values of steady-state flux are plotted as functions of temperature, speed of agitation, and feed concentration in Figs. 8, 9, and 10, respectively. Figure 8 also shows the maximum flux at different temperatures.

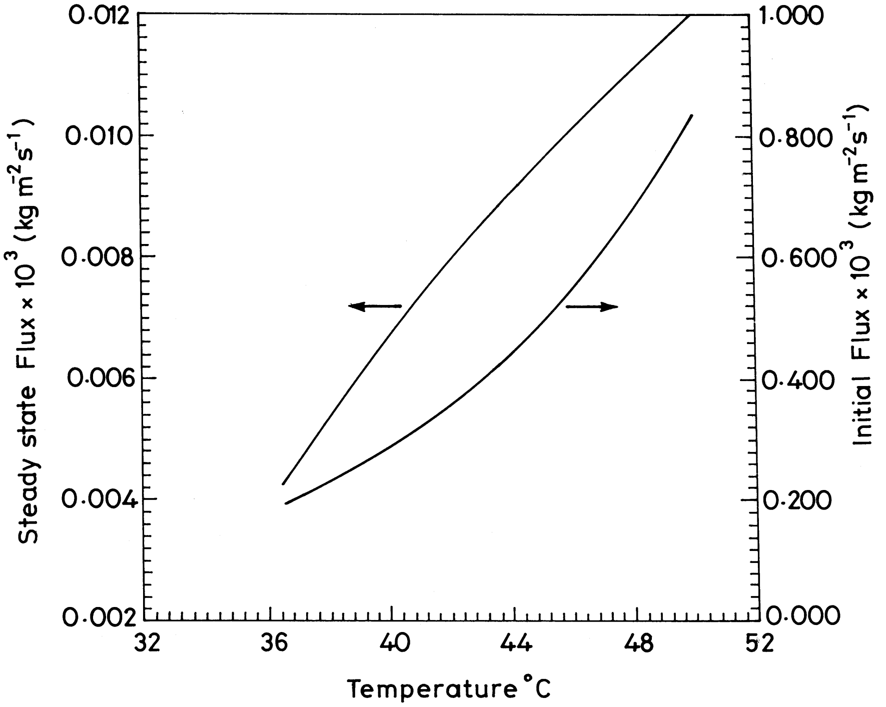

FIG. 8 Maximum and steady-state flux of water (kg·m^{-2}·s^{-1}) vs temperature (°C).

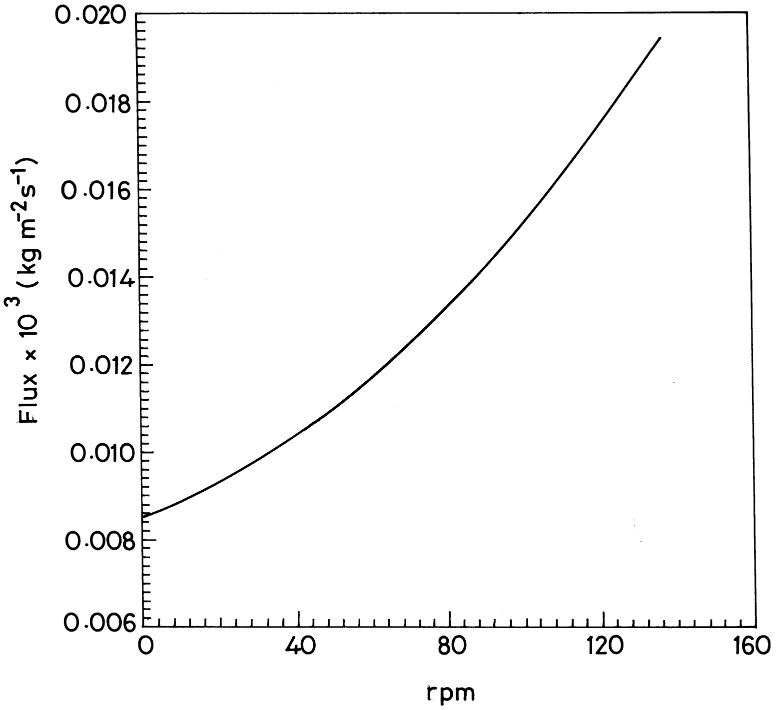

FIG. 9 Steady-state flux of water (kg·m^{-2}·s^{-1}) vs speed of agitation (rpm).

Marcel Dekker, Inc.
270 Madison Avenue, New York, New York 10016

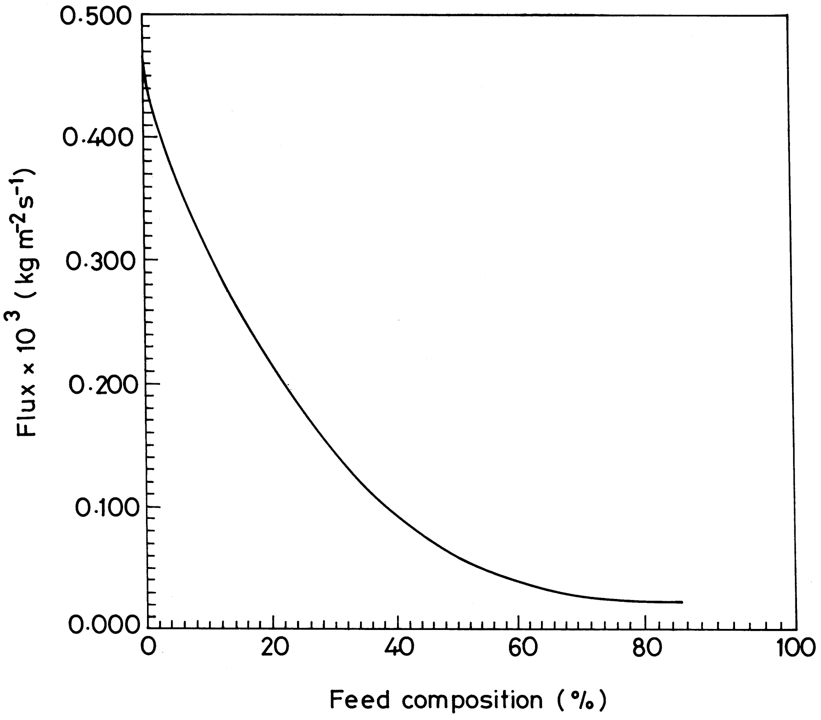

FIG. 10 Steady-state flux of water (kg·m^{-2}·s^{-1}) vs feed composition.

Effect of Presence of Salt on Rate of Permeation

In the production of water-free glycerol, the feed to the vacuum distillation column contains traces of common salt. Therefore, to study the effect of salt on the overall permeation rate, the experimental weight of product collected vs time data are plotted in Fig. 2. The figure shows the effect of sodium chloride in the solution for two different temperatures. It is evident from the graph that the rate of permeation decreases when salt is used in the feed mixture. The presence of salt reduces the vapor pressure of water in the feed mixture, thereby decreasing the overall driving force. Moreover, the salt is precipitated during the permeation of water and thereafter offers greater resistance to mass transfer.

CONCLUSION

This experimental study shows that pervaporation may be an effective method for the removal of the last trace of water from a glycerol–water mixture by using a cellophane membrane. From this study it is observed that the water selectivity of the cellophane membrane does not change with a change of the operating variables, and the selectivity coefficient of the membrane remains infinite over the range of operating variables used.

In the present case the rate of permeation is primarily controlled by the mass transfer boundary layer resistance, unlike other pervaporation systems. Thus, it can be enhanced by increasing the agitator speed and simultaneously increasing the operating temperature.

The rate of permeation in the initial period was found to be much higher than that at steady state. Therefore, the packing density (m^2/m^3) of the membrane module should be such that the entire water content can be removed in the initial period.

APPENDIX I

$$\begin{aligned}\varphi_1 = {} & \ln v_1 - g_{23} v_2 v_3 \frac{V_1}{V_2} + v_2\left(1 - \frac{V_1}{V_2}\right) + v_3\left(1 - \frac{V_1}{V_3}\right) \\ & + (g^{\mathrm{p}}_{12} v_2 + g_{13} v_3)(v_2 + v_3) - \phi_1 \phi_2 v_2 \frac{dg^{\mathrm{p}}_{12}}{d\phi_2} \\ & - \ln u_1 - \left(1 - \frac{V_1}{V_2}\right) u_2 - g^{1}_{12} u_2^2 + u_1 u_2^2 \frac{dg^{1}_{12}}{du_2} = 0\end{aligned} \tag{28}$$

$$\begin{aligned}\phi_2 = {} & \ln v_2 - g_{13} v_1 v_3 \frac{V_2}{V_1} + v_1\left(1 - \frac{V_2}{V_1}\right) + v_3\left(1 - \frac{V_2}{V_3}\right) \\ & + \left(g^{\mathrm{p}}_{12} v_1 \frac{V_2}{V_1} + g_{23} v_3\right)(v_1 + v_3) + \frac{V_2}{V_1} \phi_1^2 v_2 \frac{dg^{\mathrm{p}}_{12}}{d\phi_2} - \ln u_2 \\ & - \left(1 - \frac{V_2}{V_1}\right) u_1 - g^{1}_{12} u_1^2 \frac{V_2}{V_1} - \frac{V_2}{V_1} u_1^2 u_2 \frac{dg^{1}_{12}}{du_2} = 0\end{aligned} \tag{29}$$

SYMBOLS

C	total concentration ($kmol/m^3$)
C_w	water concentration ($kmol/m^3$)
C_0	bulk water concentration ($kmol/m^3$)
D_{wg}	diffusivity of water in glycerol (m^2/s)
E	activation energy (kJ/kmol)
f	fugacity coefficient
ΔG^E	excess free energy of mixing (kJ/kmol)
g_{kj}	Flory–Huggins interaction parameter between k and j
K	Mass transfer coefficient (m/s)
M_C	molecular weight in crosslinked unit
N_{Re}	Reynolds number

N_{Sc}	Schmidt number
N_{Sh}	Sherwood number
n	flux (kmol/m^2·s)
P^{d}	downstream pressure (N/m^2)
P^{sat}	vapor pressure (N/m^2)
R	universal gas constant (kJ/kmol·K)
T	temperature (K)
t	time (s)
u	volume fraction of component in the liquid phase
V	molar volume (m^3/kmol)
v	volume fraction of component in membrane phase
x	mole fraction in feed
y	mole fraction in permeate
z	coordinate axis along the thickness of the membrane

Subscripts

1	glycerol
2	water
3	polymer
g	glycerol
i	component
w	water

Superscripts

d	downstream interface
l	liquid feed phase
m	membrane
u	upstream interface

Greek

α	equilibrium sorption coefficient [(N/m^2)/(kmol/m^3)]
α_0	equilibrium sorption coefficient of pure water [(N/m^2)/(kmol/m^3)]
β	correction factor
ϕ	polymer free volume fraction of component in the membrane
γ	activity coefficient
δ_{c}	concentration boundary layer thickness (m)
δ_{m}	membrane thickness (m)
κ	permeability of pure water [m^3(stp)m·m^{-2}·s^{-1}(N·m^{-2})$^{-1}$]
κ_0	arrhenius constant [m^3(stp)m·m^{-2}·s^{-1}(N·m^{-2})$^{-1}$]
λ	selectivity coefficient
μ	chemical potential (kJ/kmol)

REFERENCES

1. Radovanovic, S. Thiel, and S. T. Hwang, *J. Membr. Sci.*, *48*, 55 (1990).
2. K. C. Hoover and S. T. Hwang, *Ibid.*, *10*, 253 (1982).
3. J. G. Sikonia and F. P. McCandless, *Ibid.*, *30*, 111–116 (1987).
4. F. P. McCandless and W. B. Downs, *Ibid.*
5. X. Feng and R. Y. M. Hwang, *Ind. Eng. Chem. Res.*, *36*, 1048–1066 (1997).
6. M. C. Burshe, S. A. Netke, S. B. Sawant, J. B. Joshi, and V. G. Pangarkar, *Sep. Sci. Technol.*, *32*, 1334 (1996).
7. H. Wang, X. Lin, K. Tanaka, H. Kita, and K. Okamoto, *J. Polym. Sci.*, *36*, 2247–2259 (1998).
8. H. L. Flemming, In *Proceedings of International Conference on Fuel Alcohols and Chemicals* (W. Kampen, Ed.), Charlotte, NC: K-Engineering, 1989.
9. L. Kartez, *Desalination*, *70*, 481 (1988).
10. W. Kujawski, T. Q. Nguyen, and J. Neel, *Proceedings of the Third International Conference on Pervaporation Process Chemical Industry*, 1988, pp. 355–363.
11. H. L. Fleming and C. S. Slater, "Pervaporation," in *Membrane Handbook* (W. S. W. Ho and K. K. Sirkar, Eds.), Van Nostrand Reinhold, New York, NY, 1992, Chap. 10.
12. H. E. A. Bruschke, *Proceedings of the Third International Conference on Pervaporation Process Chemical Industry*, 1988, p. 2.
13. J. Neel, Q. T. Nguyen, R. Clement, and D. J. Lin, *Ibid.*, *27*, 217 (1986).
14. R. Gref, Q. T. Nguyen, and J. Neel, *Sep. Sci. Technol.*, *27*(4), 467–491 (1992).
15. Kirk and Othmer, *Encyclopedia of Chemical Technology*, *Vol. 11*, 3rd ed., Wiley, New York, NY, 1980.
16. J. Neel, J. A. Howell (Eds.), *The Membrane Alternative*: *Energy Implications for Industry*, Elsevier Applied Science, London, 1990, p. 59.
17. A. Heintz and W. Stephan, *J. Membr. Sci.*, *89*, 143–151 (1994).
18. P. Cote and C. Lipski, *Proceedings of the Third International Conference on Pervaporation Process Chemical Industry*, 1988, p. 449.
19. A. Heintz, W. Stephan, *J. Membr. Sci.*, *89*, 153–169 (1994).
20. Rogers, Fels, and Li, *Recent Developments in Separation Science*, Vol. 2, CRC Press, Cleveland, OH, 1976.
21. P. Flory, *Principles of Polymer Chemistry*, Cornell University Press, Ithaca, NY, 1953.
22. M. H. V. Mulder and C. A. Smolders, *J. Membr. Sci.*, *17*, 289 (1984).
23. M. H. V. Mulder, T. Franken, and C. S. Smolders, *Ibid.*, *22*, 55 (1985).
24. A. Fredenslund, J. Gmehling, L. Michelsen, P. Rasmussen, and J. M. Prausnitz, *Ind. Eng. Chem.*, *Process Des. Dev.*, *16*, 450–462 (1977).
25. R. C. Reid, J. M. Prausnitz, and B. E. Poling, *The Properties of Gases and Liquids*, 4th ed., McGraw-Hill, New York, NY, 1988.

Received by editor July 8, 1998
Revision received March 1999

MARCEL DEKKER, INC.
270 Madison Avenue, New York, New York 10016

Downloaded At: 10:58 25 January 2011

Request Permission or Order Reprints Instantly!

Interested in copying and sharing this article? In most cases, U.S. Copyright Law requires that you get permission from the article's rightsholder before using copyrighted content.

All information and materials found in this article, including but not limited to text, trademarks, patents, logos, graphics and images (the "Materials"), are the copyrighted works and other forms of intellectual property of Marcel Dekker, Inc., or its licensors. All rights not expressly granted are reserved.

Get permission to lawfully reproduce and distribute the Materials or order reprints quickly and painlessly. Simply click on the "Request Permission/Reprints Here" link below and follow the instructions. Visit the U.S. Copyright Office for information on Fair Use limitations of U.S. copyright law. Please refer to The Association of American Publishers' (AAP) website for guidelines on Fair Use in the Classroom.

The Materials are for your personal use only and cannot be reformatted, reposted, resold or distributed by electronic means or otherwise without permission from Marcel Dekker, Inc. Marcel Dekker, Inc. grants you the limited right to display the Materials only on your personal computer or personal wireless device, and to copy and download single copies of such Materials provided that any copyright, trademark or other notice appearing on such Materials is also retained by, displayed, copied or downloaded as part of the Materials and is not removed or obscured, and provided you do not edit, modify, alter or enhance the Materials. Please refer to our Website User Agreement for more details.

Order now!

Reprints of this article can also be ordered at

http://www.dekker.com/servlet/product/DOI/101081SS100100231